Using Surface Topography to Re-Analyze Gradients in Mussel Byssal Threads

By

Emmie A. Ryan

Massachusetts Institute of Technology, 2015

SUBMITTED TO THE DEPARTMENT OF MATERIAL SCIENCE AND ENGINEERING IN PARTIAL FULFILMENT OF THE REQUIREMENTS FOR THE DEGREE OF

BACHELORS OF SCIENCE IN MATERIAL SCIENCE AND ENGINEERING
AT THE
MASSACHUSETTS INSTITUTE OF TECHNOLOGY

JUNE 2015

Signature of Author: Signature redacted
Department of Material Science and Engineering
May 1, 2015

Certified by: Signature redacted
Niels Holten-Anderson
Assistant Professor of Material Science and Engineering

Signature redacted

Accepted by: _____
Professor Geoffrey Beach
Professor of Material Science and Engineering
Chairman, Undergraduate Committee Chairman

Using Surface Topography to Re-Analyze Gradients in Mussel Byssal Threads

By

Emmie A. Ryan

Submitted to the Department of Material Science and Engineering
on June 1, 2015 in Partial Fulfillment of the
Requirements of the Degree of Bachelors of Science in
Material Science and Engineering

ABSTRACT

Thin film instabilities have been heavily utilized in recent years in the fields of thin film production, biology and nano-fabrication. The creation of specific wrinkling and buckling patterns has been used as both a characterization and control technique. This project aims to apply the analysis of thin film wrinkling patterns to characterize the mechanical gradient in the collagenous core fiber of mussel byssal threads. Mussel byssal threads have a natural, stiff, thin outer coating that is chemically and mechanically distinct from the softer collagenous core making them a prime subject for wrinkling analysis. Past work in the area has focused on full thread strain recovery dynamics and biochemical analysis of the collagenous and coating components in an attempt to understand the physical characteristics of the mussel byssal threads.

Thesis Supervisor: Niels Holten-Anderson
Title: Assistant Professor of Material Science and Engineering

I would like to thank my research advisor, Prof. Niels Holten-Andersen, for support, guidance and inspiration throughout this project and many others; the entire LBI group for suggestions, support and critique of the project; Prof. Thomas W. Eager for graciously allowing me to use the confocal microscope in his lab; Gregory Szeto for assistant with fluorescence confocal microscopy; Prof. Herbert Waite and the Waite Lab for providing sample materials; Prof. Lorna Gibson for academic guidance and support throughout the project and through previous semester; and Michael Tarkanian for providing training and guidance

Table of Contents

Table of Figures

Introduction and Overview

Over the past 17 years thin film buckling and wrinkling has been examined in a number of cases ranging from characterization of wrinkling of biological materials with thin coatings such as skin, fruits and arteries to the application of buckling principles to manufacture and pattern complex patterns onto nano and micro substrates without complex technology or machining. Bowden *et al.* began the examination of thin film wrinkling analysis with the by looking at thin metallic films placed on a strained PDMS substrate. Bowden *et al.* related the thermal expansion coefficient of the PDMS substrate with the stress required to initiate buckling and the wavelength of the resultant buckling through simple planar stress analysis.

This work has since been expanded in include not only planar systems but also cylindrical and spherical systems, which occur frequently in nature (ie. cells, tumors, fruits, blood vessels) and also in industry (ie. electro spun fibers, nanowires). This expansion of theory to curved surfaces allows the application of this analysis technique to be applied to mussel byssal threads which are cylindrical in shape with there length being on the order of centimeters while there radius is on the order of 100s of microns.

Mussel byssal threads are the threads used to attach the main body and shell of the mussel securely to the rocky surface of the intertidal zone in which many of the species live. The intertidal zone itself provides a mechanically challenging environment for the growth and development of life. The dynamic nature of the tide constantly flowing in and out and waves crashing applies huge amounts of stress to the creatures living in the intertidal zone while also providing them with the

nutrients they need to survive. While other creatures such as barnacles and starfish deal with this by maintaining lower profiles with broad attachment bases the mussel has developed a unique strategy that allows them to minimize attachment area while maximizing hold. The mussel produces hundreds of threads that attach inside the shell to its soft body tissue and then extend outside and bind to rocks or anything else they can attach to.

These threads have been extensively studied for their strain recovery capabilities since they can be stretched to extensive lengths, undergo a softening as physical bonds break and then recover both their original length and modulus through a self healing property even though they lack an the active repair mechanism of living tissue. Separating out the physical and chemical components of these threads has proved to be difficult owning to their small size and tough design, which protects them in the wild, but make separating the components extremely difficult.

Mussel Byssal Threads

Species and the Environment

There are numerous types of mussel species that have been studied in the past. The most common are M. galloprovincialis, M. edulis, M. californianus, P. canalicula.

Table 1: Synthesis of Information about Relevant Mussel Species

Species	Coating Thickness	Granules	Location
M. galloprovincialis	5 um (Holten-	750+/-200nm (Harrington, Masic, Holten-Andersen,	Near shore, cold waters (North Atlantic),

	Andersen, Mates, et al., 2009)	Waite, & Fratzl, 2010)	intertidal
M. edulis	Unknown	Size unknown	Near shore, cold waters (North Atlantic), intertidal
M. californianus	2-5 um (Holten-Andersen, Zhao, & Waite, 2009)	200+/-80nm (Harrington et al., 2010)	Mid to North Pacific, intertidal
P. canalicula	Graduated	none	New Zealand, subtidal

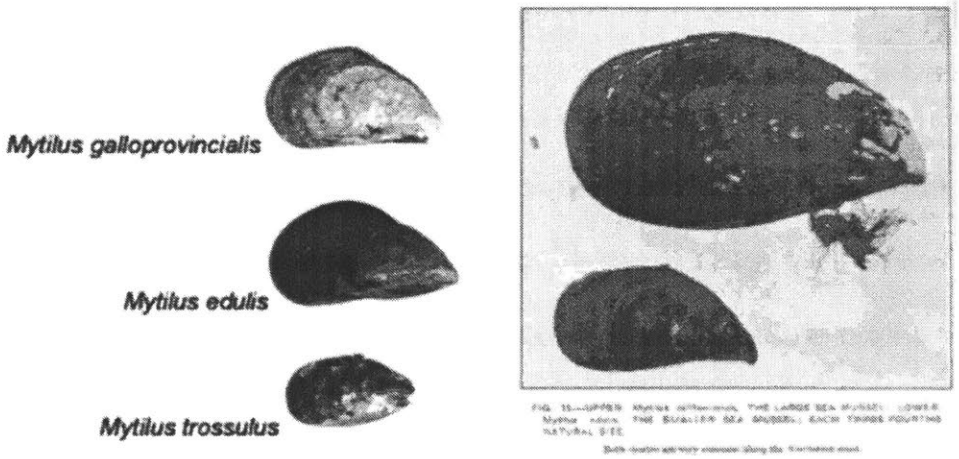

Figure 1 Comparison of size of related mussel species as found in wild populations (borrowed from (Freshwater and Marine Image Bank, 1923) and (Senckenberg Natural History Collections Dresden, n.d.)))

The byssal thread is used to connect the mussel to its substrate. Many mussel species thrive in rough intertidal zones and use a group of byssal threads to create a strong hold fast that allows them to stay put even in the dynamic wave environment. The key feature of this thread is there ability to bond soft inner tissue to the hard outer surfaces such as rocks and other shells. Inside the mussel shell is a soft body

from which emanates a group of threads that reach a few centimeter, or millimeters depending on the species, to the surface a rock. The difference in mechanical properties between these two materials poses a difficult design problem which nature has solved by creating a gradient in stiffness through out the thread to slowly transition the mechanical properties and prevent excessive stress build up in any one part of the thread. Each thread consists of two parts: the coating and the core.

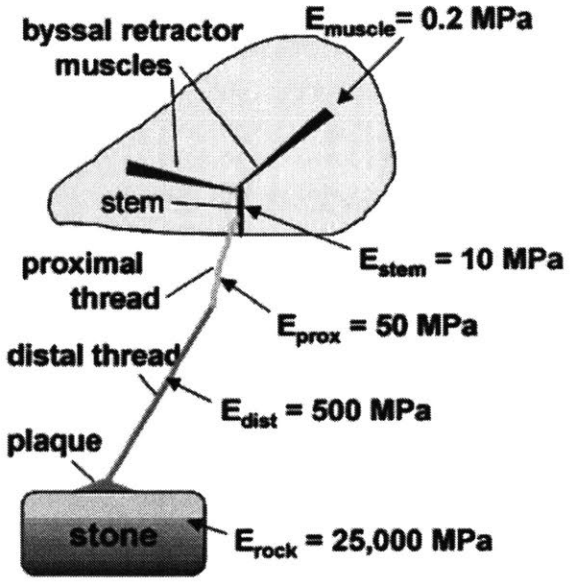

Figure 2 Simple Diagram of estimated whole thread properties and attachments (taken from (Waite, Lichtenegger, Stucky, & Hansma, 2004))

The thread itself is a composite of a softer core made of modified collagen and a thin but stiffer outer coating based on a DOPA containing protein-fatty acid mixture. The coating serves at the very least to protect the collagenous core from the multitude of bacteria that live in the ocean environment and from abrasive forces of sand and particulate matter moving around with the waves.

Coating Material

The coating material is a made up of a mixture of fatty acid molecules and a variation of a repetitive protein (mfp-1) the contains a deca-peptide sequence with modified Tyr repeats (10-15% DOPA content) (Manuscript, 2008). The sequence of DOPA repeats are thought to be the method of crosslinking between the individual proteins that lends the coatings it toughness.

Some species of mussels specifically those in the Mytilus family, including the one reported on here, also have granular structures embedded within the coating. The granules seem to be made of the same material with a different density than the bulk material. Seen below in Figure 3 (taken from (Harrington et al., 2010)) is a hypothesis presented by the group about how these granules might contribute to the stress relief and recovery of modulus mentioned earlier. They hypothesized that at the interface between the denser granules and the matrix if the material is strained recoverable coordination bonds with the DOPA side groups and included metal ions would allow the relaxation of stress and the stretching of the coating through micro tears without compromising the coating. Micro tears were observed in SEM images of strained fibers.

Harrington *et al.* also explored the density of these granules with Raman spectroscopy showing higher intensity regions of the metal-DOPA bond within the granule region lending more support to their hypothesis. Resolution is limited though with Raman techniques(Harrington et al., 2010).

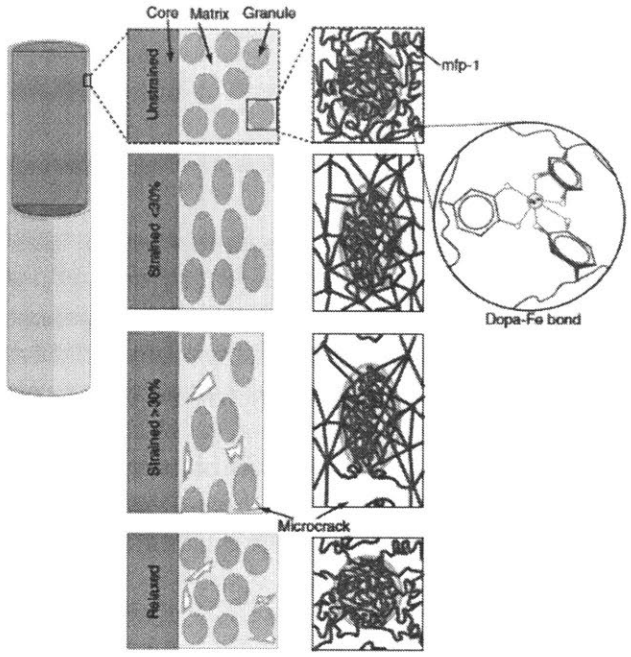

Figure 3 Possible mechanism for mechanical relaxation of the coating under stress (taken from (Harrington et al., 2010))

Core Material

The core consists of a series of modified collagen fibers that have a central collagen domain flanked by domains that are either silk-like, poly-glycine, or elastin like. The end of each collagen fiber has repeating His sequences that are thought to be the linking mechanism between the fibers which are highly oriented along the length of the fiber (Waite, et. al 2004). The variable domains in the collagen would lend the two subtypes drastically different mechanical properties neither of which accurately account for the full thread dynamics by themselves. Physically we know there must be a gradient for stress relief and biochemically it has been found that the at the proximal end, inside the shell, the elastin like, soft collagen dominates and at the distal end, attached to the rock, the silk , stiff collagen dominates. We also

know from tensile testing of the two portions of the thread there is an order of magnitude shift in the modulus of the thread from proximal to distal (see Figure 2) but the exact mechanical and biochemical gradient that occurs has not yet been well described. (Waite et al., 2004).

Unique Mechanical Properties

As alluded to above the mussel byssal thread exhibits very unique mechanical properties that make them an interesting subject for study. Past research has focused mainly on the stretching and recovery dynamics of the threads given their typical living environment. Each individual thread is able to absorb up to 120% of strain, for M. californianus, by initially deforming elastically then softens and deforms in what appears to be a plastic manner without massive fracture of the coating(Manuscript, 2008) . See Figure 4 for a diagram of a typical stress strain curve of M. galloprovincialis a closely related species.

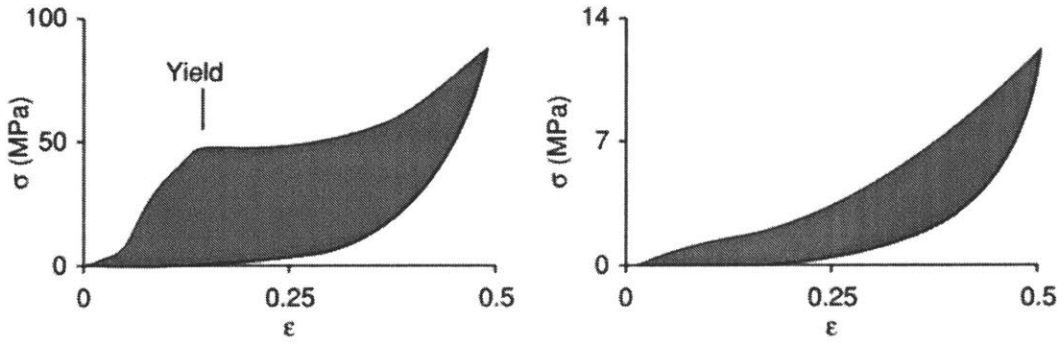

Figure 4 Hysteresis curve from the distal (left) and proximal (right) portions of a byssal thread (taken from (Waite et al. 2006))

If the fiber is then given a short period of time (less than 30 minutes) to recover in a hydrated state it will recover all the strain and re-stiffen and can then be stretched again to the same strain without any loss in modulus. This indicates some sort of self-healing dynamics that have been strongly attributed to the metal coordination bonds present in both the coating and the core material. In the past the mechanical role of the coating has been largely ignored though there is association of the strain length where the modulus decreases (ie. the fiber softens) with micro tears developing in the coating (Holten –Andersen et al., 2007).

Nano-indentation Studies

Aside from full thread mechanics nano-indentation studies were performed to get values for the for the different moduli of the coating and the core in an effort to determine the physical role of the coating. A summary of those results is presented in Table 2.

Table 2: Nano-indentation results for M. galloprovincialis (from (Holten-Andersen et al., 2007)) and estimates for M. californianus (from (Holten-Andersen, Zhao, et al., 2009))

Material	Hardness (MPa)	Stiffness (GPa) (Young's Mod.)	Ultimate Strain (%)
Cuticle (M. gallo)	100 +/- 6.2	1.7 +/- 0.1	70
Cuticle (M. cali)	100	2	70-100
Collagen (M. gallo)	20 +/- 4.0	0.4 +/- 0.09	75
Collagen (M. cali)	(1/6 of cuticle)	(1/6 of cuticle)	120
Standard Epoxies	100-150	2-3	<5

To get these measurements the threads were encased in epoxy then microtome to expose the cross sectional surface. These threads were then hydrated

in an attempt to mimic natural conditions and then nano-indentation was performed. This method of study has a number of inherent problems the first of which is the influence of the epoxy-fiber interface. Because the coating is so thin the interface effects of the epoxy binder may mask the mechanical attributes of the coating. Near the center of the thread the core material is likely outside the range of interface effect but swelling also becomes an issue. When the embedded exposed fibers are rehydrated they swell and since outward expansion is impossible vertical swelling occurs creating a domed surface that can skew nano-indentation results (Holten-Anderson, Zhao, et al. 2009).

Theoretical Background

Thin film buckling arises from a mismatch in modulus of one material deposited on top of another. The most clear cut case is the one described by Bowden *et al.* in the initial introduction of this theory which is a stiff film deposited on a soft planar substrate. In their case a metallic film deposited on a soft flexible PDMS substrate that is thermally expanded and compressed to create the in plane stress required for buckling. The simple planar case can be mathematically expanded to cases involving curved surfaces including spheres and cylinders. The sphere and cylinder are extremely common in biological settings making this an extremely useful theory for predicting and analyzing growth, physical properties and over all resultant shapes.

Thin Film Buckling of a Planar Substrate

Thin film buckling studies have been heavily utilized for characterization of planar substrates. Bowden et al. first developed the theory for a thin metallic film on a soft PDMS substrate that was subjected to thermal stresses. The energetic model correctly predicts the wavelength and buckling pattern that will arise give the stiffness and Poisson's ratios of the film and substrate and also the thickness of the film. The resultant critical stress and buckling wavelength are given by

$$\sigma_{crit} \approx 0.52\left(\frac{E_f}{(1-\nu_f^2)}\right)^{1/3}\left(\frac{E_s}{(1-\nu_s^2)}\right)^{2/3} \text{ and } \lambda \approx 4.36h\left(\frac{E_f(1-\nu_s^2)}{E_s(1-\nu_f^2)}\right)^{\frac{1}{3}} \qquad (1)$$

showing the major dependence of wavelength on film thickness and that if film thickness increases wavelength increases linearly such that the method is only applicable to the case of thin films on substrates with varying a varying stiffness.

Wrinkling in the Cylindrical Case (Basic Polar Wrinkling)

The bulk of the analysis done for this project is based of the model presented by Chen and Yin in Soft Matter 2010. Their mathematical derivation is described here with key features noted. See (Chen and Yin, 2010) for a more detailed derivation.

The system is described as a cylinder with radius R and length L (where L>>R) and overlaid by a coating thickness h. If $\Delta\varepsilon$ is the mismatch strain caused by swelling or shrinking of the substrate then the film stress of the pre-buckled state is given by

$$\sigma_{f0} = \frac{E_f E_s (2R^2 + 2Rh + h^2)\Delta\varepsilon}{2E_s(1-\nu_f^2)R^2 + [E_s(1+\nu_f) + E_f(1+\nu_s)(1-2\nu_s)](2Rh+h^2)} \quad (1)$$

where ν_s and ν_f are the Poisson's ratios of the substrate and the film respectively. If this plane stress exceeds a certain critical value a buckling mode with be induced in the film to relieve stress. This critical buckling pressure is given by

$$\rho_{cr} = \frac{\bar{E}_f\, I\, (1+\bar{K})}{R^3} \frac{(n^2-1)^2 + \bar{K}(1+\frac{AR^2}{I})}{n^2 - 1 + \bar{K} - (\bar{K}+\bar{K}^2)/n^2} \quad (2)$$

where $\bar{E}_f$ is defined as $\bar{E}_f = E_f(1-\nu_f^2)$, A and I are the cross sectional area and the moment of inertia, respectively, n is the critical wave number and $\bar{K}$ is the foundation stiffness as defined by

$$\bar{K} = \frac{\tilde{E} R}{\bar{E}_f\, h} \quad (3)$$

which accounts for effects of geometry, modulus and Poisson's ratio from both materials where $\tilde{E} = \frac{E_s}{(1+\nu_s)(1-2\nu_s)}$. If the buckling pressure is minimized with respect to n and the assumption that foundation stiffness is small compared to the wave number then a closed form solution can be found yielding

$$n_{cr} = (\frac{R}{h})^{3/4} (\frac{12\tilde{E}_s}{\bar{E}_f})^{1/4} \quad and \quad \lambda_{cr} = \frac{2\pi R}{n_{cr}} = 2\pi h\, (\frac{R}{h})^{3/4} (\frac{12\bar{E}_f}{\bar{E}_s})^{1/4} \quad (4)$$

Examining equation 4 it becomes apparent the critical wavelength is dependent not only the moduli and the Poisson's ratio of the two materials but also

heavily dependent on the curvature of the substrate. This means that the smaller the radius of the cylinder the smaller the critical buckling wavelength indicating that upon shrinking we should see a marked decrease in the wavelength of the buckling mode. It is also useful to note the effect of changing thickness of coating on the critical buckling wavelength. If all else stays the same but the thickness of the coating decreases the buckling wavelength will increase.

This model is extremely useful in predicting the wavelength of polar (along the length of the fiber) wrinkles that appear in the distal portion of the thread. The longitudinal wrinkles in the proximal portion of the thread pose more of an issue in terms of mathematical modeling.

Anisotropic Substrates and their Effects on Buckling (Longitudinal Wrinkling)

In the previous calculations it was assume the perturbation could only arise in the circumference of the fiber (polar wrinkling) and that the core material was unchanging along the length of the thread. If we instead take the approach laid out by Patrício *et al.* in which the total energy of the system is considered to calculate the wavelength of perturbation.

If we first consider a perturbation described as $u(R_1) = U \cos kz$ where k is the frequency of perturbation (assumed to be large) then the stretching energy of the shell is given by

$$F_{fs} = -\frac{\pi E_f h L R}{2(1+\nu_f)}\left[(\varepsilon_z - a) + \nu_f(\varepsilon_r - c)\right]k^2U^2$$

Where L is the length of the cylinder, R is the major radius, ε_z is the strain in the longitudinal direction, ε_r is the strain in the polar direction, k is the perturbation wavelength and U is the perturbation amplitude (all other notation carries from above. The next component that is balanced in the system is the bending energy of the film given by

$$F_{fb} = \frac{\pi E_f h^3 LR}{24(1-\nu_f^2)} k^4 U^2$$

The last energy contribution is from the elastic energy of the core material given by

$$F_s = \frac{\pi E_s L R}{4(1+\nu_s)} \sqrt{\frac{2(1-\nu_s)}{1-2\nu_s}} k U^2$$

If all the component of the energy function are then summed and the energy is minimized a critical buckling wavelength in both the polar (λ_θ^{crit}) and longitudinal (λ_z^{crit}) can be determined

$$\lambda_z^{crit} = \frac{1}{h}\left(\frac{6\tilde{E}_s}{\tilde{E}_f}\right)^{1/3} \qquad \lambda_\theta^{crit} = \frac{1}{h}\left(\frac{6\sqrt{2}\tilde{E}_s}{\tilde{E}_f}\right)^{1/3}$$

where $\tilde{E}_s = \frac{E_s}{1+\nu_s}\sqrt{\frac{2(1-\nu_s)}{1-2\nu_s}}$ and $\tilde{E}_f = \frac{E_f}{1-\nu_f^2}$. Data is run through both models for the polar wrinkling case for comparison.

Using Wrinkling to Analyze Mechanical Gradients

The use of wrinkling in the analysis of changing mechanical gradients of the substrate material has been shown to work in previous studies. A group at NIST presented the example that most closely matches the goal of this project in 2006, they used a film with a known modulus and thickness to probe the mechanics of an underlying soft material gradient. They also confirmed their findings by matching the calculated modulus to the bulk modulus found by indentation of the individual gradient sections.

It is useful to note from the image below that there is a gradual shift in wrinkle orientation as well as periodicity. If you look closely at the difference in modulus between the first and last image you will see a difference in stiffness that is about an order of magnitude. This correlates well with the mussel fiber's difference in modulus between the proximal and distal end. Wilder et al. correctly predicted the Young's modulus of each section of the gradient by using simple linear elastic models and the buckling periodicity similar to the model presented below for this analysis.

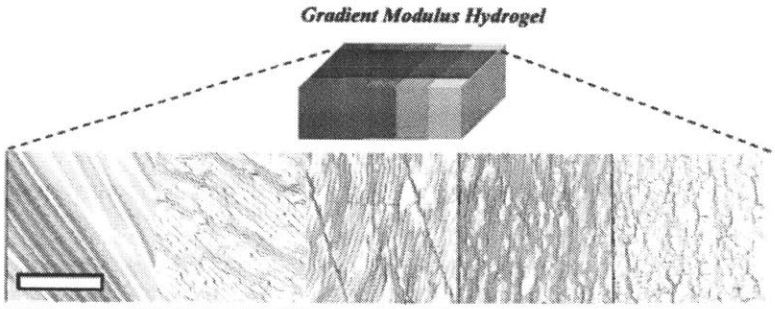

Zone	1	2	3	4	5
Cross-linker	0.5 %	1 %	2 %	4 %	8 %
E, (MPa)	0.56 MPa	0.81 MPa	1.2 MPa	2.0 MPa	2.6 MPa
σ (MPa)	± 0.06 MPa	± 0.07 MPa	± 0.06 MPa	± 0.43 MPa	± 0.51 MPa

Figure 5 Showing the difference in wrinkling pattern as the modulus of the underlying material shifts (taken from (Wilder, Guo, Lin-gibson, Fasoka, & Stafford, 2006))

Methods and Data

To utilize the model described above a simple technique based on hydration and dehydration of the fibers was developed to apply the strain needed to observe buckling or wrinkling behavior. Optical microscopy was then used to examine the wrinkling patterns and analysis was done to fit wrinkling data to past data obtained through nano-indentation.

Material Selection

Hydrated, detached fibers were received from Waite Research Lab at the University of California Santa Barbra. The received threads are from mussels grown in tanks under replicated ocean conditions. They were received cut from the stem and stored in synthetic seawater. The species that was studied in this report was the *Mytilus californianus*, which inhabits intertidal zones of the western coast of the United States. This species is optimal due to its long byssal threads, distinct core-shell structure and its well studies mechanics in past research.

Hydration and Dehydration Method

The simplest way to induce planar stress in the coating to induce buckling is simply though shrinkage from dehydration. These threads typically exist in their swelled state owning to the fact that there are almost constantly submerged or at least wet in their natural environment. When dried the threads shrink significantly in the radial direction and less so in the longitudinal direction-inducing hoop and compressional stresses into the thin film coating. The buckling that results from the stresses can then be observed with optical microscopy.

For this project the hydrated fibers were taken out of the water solution they came in and placed on a clean glass substrate. They were quickly examined to check that they had both proximal and distal portions which are visually distinctive. Threads that did not contain both components were discarded. The full threads were removed one at a time from the solution and secured at both ends with a small amount of modeling clay. The imaging points were then marked at semi-regular intervals with a permanent marker on the glass. See Figure 6 a reference image of a typical testing setup.

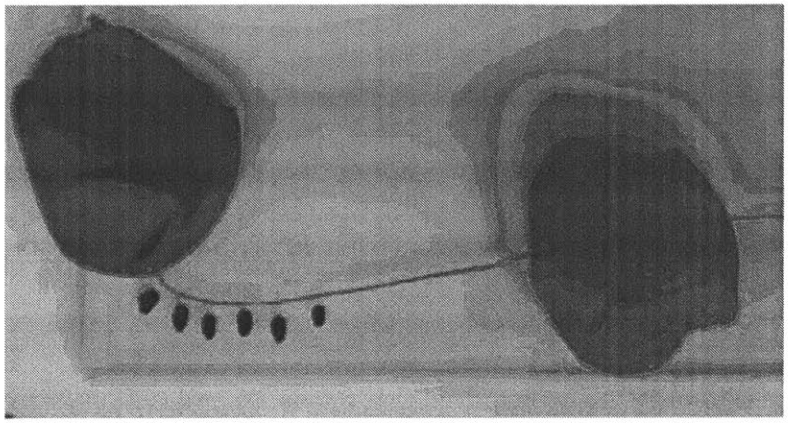

Figure 6 M. californianus thread secured and marked for imaging

Once the fibers were securely placed on the glass a small amount of water was placed around the fiber to keep it hydrated while the imaging process was taking place. The fibers were then imaged using a Hirox KH-8700 laser confocal microscope with a 10x lens attachment at the lowest magnification. The laser confocal was chosen due to its capabilities of digitally incorporating multiple images at varying focal lengths to properly image highly varied surface features. The 3D Hirox imaging software was used to create the imaging in situ.

After the fibers were measured in a hydrated state all the excess water was absorbed with a paper towel without disturbing the positioning of the thread. The thread was then give 10 minutes to dry completely and placed back under the microscope. The imaging points marked at the beginning were then reexamined to place images in as close to the same are of the fiber as possible. Once the fibers were imaged both wet and dry they were placed back in the seawater solution for future reference if needed.

Distal (Polar) Wrinkling Data

Data was collected using the method described above and calculations for the modulus of the coating were conducted using a Young's modulus for the core being 0.5GPa from the nano-indentation data, a Poisson's ratio for the coating chosen to be 0.35. This value was arbitrarily chosen since it was the most commonly used in model systems but varying it from 0.35-0.49 seems to have little to no effect on the final calculated value (Chen and Yin, 2010). The Poisson's ratio for the core material on the other hand was chosen to be 0.49 which is as close to incompressible as allowed by the model this does seem to have a significant effect on the final values so it is possible that this is source of error if the core is in fact not an incompressible material. Though these calculations are based on the simplified first model examination of the second model presented used to calculate the longitudinal wrinkling pattern shows that if the soft core is nearly incompressible and the outer shell is quite stiff then polar wrinkling is favored as is seen in the distal portion of the thread (Patrício et al., 2014)

The thickness of the coating was assumed to be a uniform 5μm in the entire distal portion of the thread. Only the hydrated measurements were considered in the final calculation of the coating stiffness. Cross sectional images of the fibers under going the drying process indicate that towards the end of the process the fibers under go so much shrinkage that the cylindrical shape is no longer maintained this translates into irregular radii which in turn greatly affects the model depending on which radius is measured for the dry fiber. This over shrinkage from drying likely accounts for the huge amount of variability and the constant underestimation

for the dry modulus. See supplementary images for example of over drying case and sample of the data from the polar wrinkling calculations.

Proximal (Longitudinal) Wrinkling Data

For the proximal portion of the thread the second mathematical method presented above was used for analysis. This model shows (see Patrício *et al.*) that in the case where the strain in the longitudinal direction (ε_z) is greater than or equal to strain in the polar direction (ε_r) longitudinal wrinkles will arise instead of polar wrinkles. If we assume the coating is the same stiffness through out since it is the same composition and microstructure the data from the polar wrinkling calculation can then determine the core stiffness variation in the proximal section by tracking changes in wavelength.

The Poisson's ratio of the core structure was again assumed to be 0.49 to be self-consistent with the above calculations. The modulus of the coating material was taken to be 2.36GPa as calculated from the distal portion of the thread. The coating thickness was taken to be 2μm from observations of thinner coating thickness in proximal regions (Holten-Andersen, unpublished findings).

Conclusions

The Distal Region

The data obtained from examining the distal portion of the threads in their hydrated state indicates that the stiffness of the coating is 2.36±0.45 GPa, which is close to but slightly higher than the value measured for the nano-indentation

studies which centered on 2GPa for the M. californianus. These calculations are based of nano-indentation results from the internal core material, which we can assume are accurate enough due to the careful testing procedure employed to acquire them.

The Transitional Region

The original goal of this project was to be able to probe a continuous gradient from proximal to distal which should be entirely possible given the theoretical model presented for the longitudinal case which can also be applied to the polar case though is more complicated. The issue with probing the gradient more precisely is an imaging and repeatability one. Each individual fiber varies in the length of its proximal and distal sections, its' over all diameter and perhaps even the thickness of the coating. It has been observed that the coating is closer to 2μm near the proximal portion and 5μm near the distal portion. Those measurements were used to perform the calculations above but the actual variability in coating thickness has not been extremely well measure due to the difficult of producing sample in which the thickness could be reasonably measured.

The transitional region poses the most problems in that it is typically only 200-400μm in length and while we do see a transition from longitudinal to polar wrinkling the pattern changes too rapidly to gather real significant data on at that level since the longitudinal wrinkles are increasing in wavelength (up to 60-70 μm by the transitional region) and the polar wrinkles have not yet become readily apparent (λ=90-100 μm) to measure accurately. The most that can be said is that the

entire shift from soft proximal region core material to stiff distal region material occurs in the 200-400μm as the data is self consistent on either side of the region.

The Proximal Region

There are two interesting points to be made about the proximal portion of the thread. The first has to do with the preexisting wrinkles in the hydrated (natural) case. The fact that a periodic wrinkling pattern already exists suggest that during the processing of the fiber the pattern must have been developed. The fibers themselves are created through a sort of injection molding like process where the precursors are injected into a groove in the soft tissue which is then touched to the substrate outside the shell and the pulled back in revealing a newly created thread.

Some tension must be generated during this process inducing a strain that is higher in the softer portion of the thread. The coating likely sets and is bonded to the corea and this point and once the thread has relaxed back to its normal state it is put under compressive stress due to shrinkage in the longitudinal direction. According the model presented by Patrício *et al.* would induce the longitudinal wrinkling seen in the original threads. If it was possible to stretch the threads then image the wrinkles in the stretched state I suspect that they would disappear. The strain at which they disappear could also then be used to back out the original tension that the thread is under directly after creation assuming the coating and core do not 'harden' over time. This experiment was not conducted due to the physical difficulty of straining and imaging the fibers in their hydrated state.

The second point is that the wrinkling patterns do in fact show a shift of stiffness in the underlying substrate from proximal to distal ranging from 3.6MPa to

333.31 MPa measured as the highest value before the wrinkles became indistinguishable in the transitional region. These numbers fit well with the estimate stiffness values of the core material from full thread dynamics. A more careful study of relating exact position along the thread to the gradient in stiffness would be useful but the difficultly lies in the massive amount of variation between thread lengths in relation to their position on the stem. If full-uncut threads still attached to the stem could be obtained it could potentially be shown for a few threads the exact nature of the gradient of the underlying core material.

Interface Dynamics

The chemistry and dynamics of the coating and the core are at this point completely unknown. The models used above both rely on a non-slip boundary condition at the interface to produce periodic buckling from strain mismatch. Up to this point we have just assumed that this is the case in the byssal thread but this assumption warrants further examination. A very recent study done by Stoop and Müller suggest that we may be able to tell whether or not there is slipping at the interface by looking at the morphology of the wrinkles themselves. They show that in the case of a sliding boundary between a stiff film and rigid cylindrical substrate that instead of getting period wrinkling as a result of the film will buckle then fold to dissipate strain energy. This effect can be seen in sliding a a sleeve up your arm the material will first buckle up then under further stress fold over back on itself (Stoop and Müller 2015). Out of all the fibers and images observed for this project I did not once observe this type of behavior suggesting that the interface is in fact a non-slip

interface. This conclusion is further supported by the fit of the data with the numerical models presented above.

The exact bonding method is currently unknown but one possible source could be an interaction and chemical bonding of the DOPA moieties in the coating and the histidine end groups of the collagenous core components. It has been shown that a bond between these two groups contributes to the scleratization of squid beaks. This process of crosslinking DOPA and histidine occurs in a non-specialized seawater environment suggesting that it would be entirely possible for this to occur in the native mussel environment (Misezer et al. 2010).

Testing for the presence of this cross link has proved difficult due to the small nature of the threads and the extreme resistance of the coating to any treatment that would allow it to be removed without damaging the core material. Raman spectroscopy could potential be used to search for a histidine-DOPA marker at the interface which if present would provide strong additional evidence that the interface is in fact tightly bonded giving lending more support to the use of thin film buckling as an analysis technique.

Works Cited

Bowden, N., Brittain, S., Evans, A.G., Hutchinson, J.W., Whitesides, G.M. (1997). Spontaneous formation of ordered structure in thin films of metals supported on an elastomeric polymer.

Stoop, Norbert and Müller, Martin Michael
2015 Non linear buckling and symmetry breaking of a soft elastic sheet sliding on a cylindrical substrate. International Journal of Non-linear Mechanics. Feb 2015. DOI: 10.1016/j.ijnonlinmec.2015.02.013

Misezer, Ali; Rubin, Daniel; Waite, Herbert J.
2010 Cross-linking Chemistry of a Squid Beak. Journal of Biological Chemistry. Sept 2010. DOI: 10.1074/jbc.M110.161174

Freshwater and Marine Image Bank. (1923). Photo M. cali and M. edulis. University of Washington Libraries Digital Collections. Retrieved from http://eol.org/data_objects/19678799

Harrington, M. J., Masic, A., Holten-Andersen, N., Waite, J. H., & Fratzl, P. (2010). Iron-clad fibers: a metal-based biological strategy for hard flexible coatings. *Science (New York, N.Y.)*, *328*(5975), 216–20. doi:10.1126/science.1181044

Holten-Andersen, N., Fantner, G. E., Hohlbauch, S., Waite, J. H., & Zok, F. W. (2007). Protective coatings on extensible biofibres. *Nature Materials*, *6*(9), 669–72. doi:10.1038/nmat1956

Holten-Andersen, N., Mates, T. E., Toprak, M. S., Stucky, G. D., Zok, F. W., & Waite, J. H. (2009). Metals and the integrity of a biological coating: the cuticle of mussel byssus. *Langmuir : The ACS Journal of Surfaces and Colloids*, *25*(6), 3323–6. doi:10.1021/la8027012

Holten-Andersen, N., Zhao, H., & Waite, J. H. (2009). Stiff coatings on compliant biofibers: the cuticle of Mytilus californianus byssal threads. *Biochemistry*, *48*(12), 2752–9. doi:10.1021/bi900018m

Manuscript, A. (2008). Mussel-designed Protective Coatings for Compliant Substrates. *J. Dent. Res.*, *87*(8), 701–709.

Miserez, A., Rubin, D., & Waite, J. H. (2010). Cross-linking chemistry of squid beak. *The Journal of Biological Chemistry*, *285*(49), 38115–24. doi:10.1074/jbc.M110.161174

Patrício, P., Teixeira, P. I. C., Trindade, a. C., & Godinho, M. H. (2014). Longitudinal versus polar wrinkling of core-shell fibers with anisotropic size mismatches. *Physical Review E*, *89*(1), 012403. doi:10.1103/PhysRevE.89.012403

Senckenberg Natural History Collections Dresden. (n.d.). M. gallo, M. edulis, M. trossulus. Retrieved from http://www.senckenberg.de/root/index.php?page_id=5090&PHPSESSID=1tquea4joid4mvkkvt06h7jaaem1jqlg

Szeto, G. (n.d.). Hydrated Fiber Images (1). *Lab Notes*, 3–5.

Waite, J. H., Lichtenegger, H. C., Stucky, G. D., & Hansma, P. (2004). Exploring molecular and mechanical gradients in structural bioscaffolds. *Biochemistry*, *43*(24), 7653–62. doi:10.1021/bi049380h

Waite, J. H., Weaver, J. C., & Vaccaro, E. (2006). Mechanical Consequences of Biomolecular Gradients in Byssal Threads. *Bionanotechnology, Chapter 3*, 25–37.

Wilder, E. A., Guo, S., Lin-gibson, S., Fasolka, M. J., & Stafford, C. M. (2006). Measuring the Modulus of Soft Polymer Networks via a Buckling-Based Metrology. *Macromolecules*, *39*, 4138–4143.

Yin, J., Bar-Kochba, E., & Chen, X. (2009). Mechanical self-assembly fabrication of gears. *Soft Matter*, *5*(18), 3469. doi:10.1039/b904635f

Supplementary Materials

Sample of Data from Longitudinal Buckling

Fiber #	Calculated Modulus (dry)	Calculated Modulus (wet)
2	0.265	None
	0.693	None
	0.9924	None
3	1.749	none
4	1.799	2.229
5	0.287	none
	0.141	2.538
6	2.427	None
	10.753	none
7	1.128	2.456
	1.370	None
	2.00	2.811
8	0.809	1.524
	0.266	2.612
11	0.117	None
	0.634	None
12	0.436	none

*fibers and measurements that were clearly outside the normal range (below 0.1GPa or above 10GPa were excluded)- errors assume to have arisen from measurement mistakes or unclear imaging

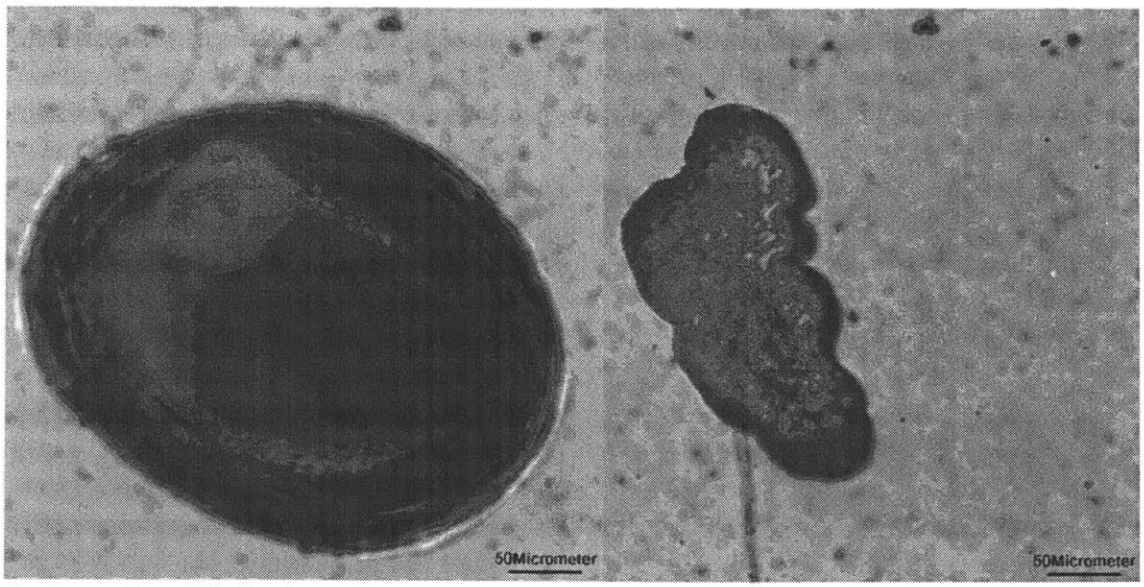

Hydrated and Dehydrated cross section of M. californianus showing serious loss of cylindrical shape upon final drying